Phonon dynamics in type-VIII silicon clathrates: Beyond the rattler concept

Payam Norouzzadeh,[1] Charles W. Myles,[2] and Daryoosh Vashaee[1]
[1]*Department of Electrical and Computer Engineering, Monteith Research Center, North Carolina State University, Raleigh, North Carolina 27606, USA*
[2]*Department of Physics, Texas Tech University, Lubbock, Texas 79409-1051, USA*
(Received 16 November 2016; revised manuscript received 25 March 2017; published 11 May 2017)

Clathrates can form a type of guest-host solid structures that, unlike most crystalline solids, have very low thermal conductivity. It is generally thought that the guest atoms caged inside the host framework act as "rattlers" and induce lattice dynamics disorders responsible for the small thermal conductivity. We performed a systematic study of the lattice dynamical properties of type-VIII clathrates with alkali and alkaline-earth guests, i.e., X_8Si_{46} (X = Na, K, Rb, Cs, Ca, Sr, and Ba). The energy dependent participation ratio (PR) and the atomic participation ratio of phonon modes extracted from density functional theory calculations revealed that the rattler concept is not adequate to describe the effect of fillers as they manifest strong hybridization with the framework. For the case of heavy fillers, such as Rb, Sr, Cs, and Ba, a phonon band gap was formed between the acoustic and optical branches. The calculated PR indicated that the fillers suppress the acoustic phonon modes and change the energy transport mechanism from propagative to diffusive or localized resulting in "phonon-glass" characteristics. This effect is stronger for the heavy fillers. Furthermore, in all cases, the guest insertion depressed the phonon bandwidth, reduced the Debye temperature, and reduced the phonon group velocity, all of which should lead to reduction of the thermal conductivity.

DOI: 10.1103/PhysRevB.95.195206

I. INTRODUCTION

Clathrate semiconductors are among novel materials with excellent potential to fulfill the phonon-glass electron-crystal (PGEC) concept. These caged structure materials contain guest atoms which are believed to vibrate at very low frequencies inside the cages and scatter the acoustic phonons of the host and thereby lower the thermal conductivity. It is frequently stated that because the filler-host atomic bonding is weak, the presence of the fillers usually has little effect on the host electronic bands, so that the filler reduces the thermal conductivity without impairing the electrical properties [1]. Although, the rattler hypothesis is the most popular mechanism in explaining the behavior of the clathrates and skutterudites, the impact of the fillers on the lattice dynamical properties is not fully explained and yet remains an open question. Some observations such as the localized modes seen in inelastic neutron scattering and heat capacity measurements support empirically the rattling concept in skutterudites [2,3]. However, the inelastic neutron scattering (INS) experiments on Fe_4Sb_{12} containing Ce or Le filler indicated evidences for the existence of coherent propagation of filler phonons [4], which is inconsistent with the rattler concept. The INS studies of phonon dynamics in (La,Ce)Fe_4Sb_{12} skutterudites revisited the picture of rattling fillers in a host cage and the microscopic mechanism responsible for the scattering of heat carrier phonons. Furthermore, the results from the theoretical studies are also contradicting. The rattling behavior implies a resonant scattering resulting from the weak interaction between the filler atoms and the cage atoms, which is different from the conventionally postulated anharmonic scattering in the empty structures. In contrast to the rattling concept, Feldman *et al.*, using lattice dynamic calculations, explained the suppression of the thermal conductivity in (La,Ce)Fe_4Sb_{12} by the strong interaction of the fillers with the heat carrying phonons of the host framework [5]. The results of the molecular dynamics (MD) simulations are also rather confusing. For example, Bernstein *et al.*, using MD calculations, found that the reduced thermal conductivity of filled skutterudites is due to the anharmonic interaction between the filler and the host atoms [6], while Huang and Kaviany, also using MD calculations, showed that the reduced group velocity is responsible for the reduction of the thermal conductivity in $Ba_x(CoSb_3)_4$ [7]. In another study, Zebarjadi *et al.* showed using the MD simulations that filler atoms of a filled skutterudite lead to smaller phonon group velocity and therefore, reduce the thermal conductivity [8].

There are also a few reports on the influence of fillers in clathrates and, again, the results are conflicting. Ritchie *et al.* found a complicated interaction between the Na fillers and the Si_{136} framework. In fact, Na_xSi_{136} allows the existence of both rattling and tight-fitting fillers. When the Na atoms are inside the larger Si_{28} cage, which can happen at both low and high Na concentration, they behave as rattling fillers. However, when they are inside the smaller Si_{20} cage, which happens at high Na concentration, they show tight-fitting behavior. For $x \leqslant 9$, the thermal conductivity decreases upon Na filling, and for $x > 9$, the thermal conductivity increases mostly due to the increment of the electronic part of the thermal conductivity while the lattice part of the thermal conductivity remains almost unchanged. The reported phonon group velocity data showed that as the occupancy of Na atoms increases, the phonon group velocity fluctuates and does not present a clear trend [9]. Euchner *et al.* performed a high-resolution inelastic neutron scattering study of the lattice dynamics in the clathrate system Ba-Ge-Ni and suggested that the phononic filter effect, which originates from both the structural complexity of the framework and the specifically bonded filler atoms, is responsible for the low lattice thermal conductivity [10]. However, according to the results by Christensen *et al.*, the principal effect of the filler atoms in type-I clathrate $Ba_8Ga_{16}Ge_{30}$ (BGG) is to reduce the group velocity of the acoustic phonons

due to the avoided crossing of the phonon modes [11]. Later, Tadano *et al.* analyzed BGG by first-principles calculations and observed a tenfold reduction in the phonon relaxation time due to the rattlers. They found that the phonon scattering in BGG is nonresonant and the change in the phonon group velocity is less significant [12]. Interestingly, Pailhès *et al.* showed recently that the interaction between the fillers and the framework atoms in type I Ba_8Si_{46} is a purely harmonic process and leads to localization of the propagative phonons; hence, transforming the phonon transport into a diffusivelike regime [13].

Recently, there have been several theoretical studies of the structural, electronic, elastic and various transport properties of the type VIII silicon clathrates [1,14]. Our previous studies also predicted that these hypothetical materials should possess a large thermoelectric power factor [15]. However, there have been little investigation of their vibrational properties and even fewer studies of their thermal properties so far. For the discussed reasons, the fillers may or may not have significant effect on thermal transport properties depending on their vibrational characteristics. Therefore, adopting a rigorous first-principles approach for addressing accurately the aforementioned issues and the role of the fillers in these structures is necessary.

In this study, we present the results of a first-principles theoretical study of lattice dynamical properties of the Si- type VIII clathrates filled with a group of alkali and alkaline earth atoms. We have previously shown that Li, Be, and Mg fillers result in metallic clathrates [14]. We have, therefore, studied the semiconducting clathrates including Na_8Si_{46}, K_8Si_{46}, Rb_8Si_{46}, Cs_8Si_{46}, Ca_8Si_{46}, Sr_8Si_{46}, and Ba_8Si_{46}. We have analyzed, using first-principles calculations, the actual role of the fillers on the lattice dynamical properties of these clathrate materials and report the phonon bandwidth, and the phonon group velocity. In particular, our results indicate (a) how loading the fillers into Si framework affects the phonon group velocity, (b) which filler has the largest effect, and (c) to what degree the phonon modes in these materials are localized and what their heat transfer characteristics are. We will specially focus on the Ba_8Si_{46} system as the representative of type VIII clathrates filled by either alkali or alkaline earth atoms.

II. COMPUTATIONAL PROCEDURE

The details of DFT calculations and the procedure to obtain elastic properties are presented here. The calculations include phonon dispersions, partial phonon density of states (DOS), participation ratios, and atomic participation ratios for type-VIII binary clathrates Na_8Si_{46}, K_8Si_{46}, Rb_8Si_{46}, Cs_8Si_{46}, Ca_8Si_{46}, Sr_8Si_{46}, and Ba_8Si_{46}.

A. DFT calculations

First-principles density functional theory (DFT) calculations were performed using the VASP code [16], which uses the projector augmented wave (PAW) method and the generalized gradient approximation (GGA). The lattice constants of the unit cells containing 54 atoms along with the internal coordinates were relaxed so that the force convergence threshold of 10^{-4} eV $Å^{-1}$ was satisfied to ensure high accuracy of the ground state. The cutoff energy of 400 eV was employed for all structures. The Perdew- Burke- Ernzerhof (PBE) exchange-correlation functional [17] was used. The Brillouin-zone integration was achieved with a ∼0.17 per Å k spacing, which leads to a $5 \times 5 \times 5$ Monkhorst-Pack mesh [18]. The k mesh was forced to be centered on the gamma point. The first-order Methfessel-Paxton smearing with a width of 0.2 eV was employed [19]. Finite-displacement or the so-called frozen phonon method was employed. One drawback of the frozen-phonon method is that large supercells are needed to accurately calculate the force constant matrix. However, considering the large unit cell of the clathrates, the supercell is often not necessary [12,13,20]. After obtaining the ground state, the Hellman-Feynman forces were calculated by displacing the asymmetric atoms by ± 0.01 Å while no significant dependence on the displacement value was observed. Then, the dynamical matrices were determined from the calculated forces by the PHONON package as implemented in the MEDEA software [21,22].The harmonic approximation was employed to determine the phonon dispersion spectrum by solving the dynamical matrices for the specified wave vectors.

B. Elastic properties

A complete set of single-crystal elastic constants are needed to obtain the elastic properties of a material. For the case of cubic crystal, three elastic stiffness constants C_{11}, C_{12}, and C_{44} are required. By straining the lattice at fixed volumes, these three constants C_{ij} were extracted [23]. The free energy were calculated then as a function of the strain. The bulk modulus B and tetragonal shear modulus C' were calculated from three independent C_{ij} as

$$B = \frac{C_{11} + 2C_{12}}{3} \quad \text{and} \quad C' = \frac{C_{11} - C_{12}}{2}. \tag{1}$$

C' was obtained by applying the following strains [24]:

$$\varepsilon = \begin{pmatrix} \delta & 0 & 0 \\ 0 & \delta & 0 \\ 0 & 0 & (1+\delta)^{-2} - 1 \end{pmatrix}, \tag{2}$$

in which δ is the magnitude of the strain. The Helmholtz free energy of the strained structure $F(\delta)$ is a function of the applied strain δ as $F(\delta) = F(0) + 6C'V\delta^2 + \mathrm{O}(\delta^3)$, where V and $F(0)$ are the volume and the free energy of the unstrained structure, respectively. C_{44} was determined by applying the following stress [23]:

$$\varepsilon = \begin{pmatrix} 0 & \delta & 0 \\ \delta & 0 & 0 \\ 0 & 0 & \delta^2/(1-\delta^2) \end{pmatrix}, \tag{3}$$

in which the free energy is obtained as $F(\delta) = F(0) + 2C_{44}V\delta^2 + \mathrm{O}(\delta^4)$. The shear modulus was determined as the solution of the Hershey-Kroner relation [25,26]. The average shear modulus G_{H} was calculated per Hill modulus $G_{\mathrm{H}} = 1/2(G_{\mathrm{R}} + G_{\mathrm{V}})$ [27] where G_R and G_V were determined by the following relations [28]:

$$G_R^{-1} = \tfrac{2}{5}C'^{-1} + \tfrac{3}{5}C_{44}^{-1}, \quad G_V = \tfrac{2}{5}C' + \tfrac{3}{5}C_{44}. \tag{4}$$

Young's modulus E is a function of bulk and shear moduli, i.e., $E = 9BG/(3B + G)$. Given the bulk and the shear moduli, the longitudinal V_l and the transversal

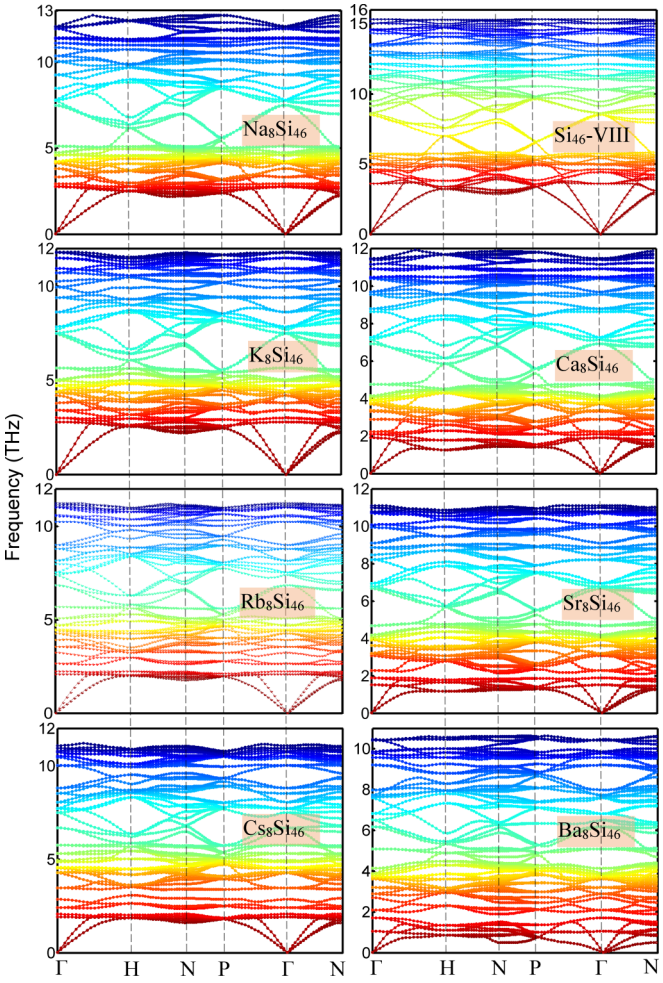

FIG. 1. The phonon dispersion of filled X_8Si_{46}-VIII clathrate structures, where X = Na, K, Rb, Cs, Ca, Sr, and Ba. Colors are for better visualization and have no particular meaning.

V_t sound velocities were calculated using the following relations [29]:

$$\rho V_l^2 = B + \tfrac{4}{3}G, \quad \rho V_t^2 = G, \tag{5}$$

where ρ is the mass density. The average speed of sound and Debye temperature were finally determined by [30]

$$V_s^{-3} = \frac{1}{3}\left(\frac{1}{V_l^3} + \frac{2}{V_t^3}\right), \quad \theta_D = \frac{hV_s}{k_B}\left[\frac{3}{4\pi}\left(\frac{N_A\rho}{M}\right)\right]^{\frac{1}{3}}, \tag{6}$$

where h, k_B, N_A, and M are Planck's constant, Boltzmann's constant, Avogadro's number, and average molecular weight, respectively.

III. RESULTS AND DISCUSSION

A. Phonon dispersion and phonon density of states

The phonon dispersion of the filled X_8Si_{46}-VIII clathrate structures (X = Na, K, Rb, Cs, Ca, Sr, Ba) are presented in Figure 1. It can be seen that as the atomic mass of the filler increases, phonon gaps are formed above the acoustic phonon modes region. For the case of light fillers, Na, K, and Ca, no phonon gap is observed. In contrast, the heavy fillers Rb, Cs, Sr, and Ba develop gaps, respectively, within 2.34–2.7, 3.07–3.37, 1.89–2.09, and 1.7–1.88 THz frequency windows, cut through the acoustic phonons of the framework, and demonstrate the avoided crossing effect. Moreover, the slope of TA and LA modes decrease with the mass of the filler while Ba atom shows the largest decrement in the phonon group velocity. In addition, the phonon bandwidth is compressed upon loading the fillers, and as the atomic mass raises the compression increases. The Ba filled system presents the largest downward shift of the phonon modes. In Ba_8Si_{46}-VIII, the phonon bandwidth is significantly decreased (by ∼33% from 15.2 THz to 10.4 THz), which means that the number of accessible heat conducting channels is limited upon loading the filler in the cage, which is more significant for the heavier Ba filler. The bandwidth reduction amounts to ∼57% for the acoustic phonon modes which contribute the most in the heat conduction process. It can be seen that Ba introduction has reduced the acoustic modes bandwidth to ∼1.8 THz while in empty Si_{46}-VIII the corresponding bandwidth extends up to ∼3.5 THz. These plots clearly manifest that the slopes of the acoustic phonon modes decrease as the filler occupies the void sites inside the framework, which is more significant for the heavier atoms. The reduction of phonon bandwidth and phonon group velocity occurs for all the alkali and alkaline earth atoms as presented in Fig. 1. The phonon gaps for the case of Ba, Rb, Cs, and Sr fillers are at low frequency around 2 THz. The gaps limit the available phonon states at low frequencies corresponding to the heat carrying acoustic phonon modes; hence dissipate the energy of phonons in that frequency window and flatten the phonon dispersion curves. For the case of Si_{46}-VIII, there are only two phonon band gaps in the optical phonon region within 11.77–11.93 and 12.16–12.40 THz frequency range. The insertion of Ba into the Si_{46} framework creates a gap in the frequency range of 1.7–1.88 THz, which cuts through the acoustic phonon modes of Ba_8Si_{46}-VIII. There can be two explanations for the formation of phonon band gaps. First, the heavy guest atom placed inside the cage can be viewed as a periodic 3D lattice of identical high-density spheres inside a low-density host material. It has been theoretically shown that such a periodically variable density gives rise to a phononic band gap [31]. As the mass ratio increases, the band gap also increases [32]. Second, the avoided crossing between the host acoustic modes and the rattler localized modes can lead to the formation of phonon band gaps [11,33]. A close inspection of the vibrational eigenvectors of Ba_8Si_{46}-VIII also revealed that the symmetry avoided crossing, which resulted from loading Ba atoms, occurs several times. For the TA modes, avoided crossings occur at ∼0.75 THz along the Γ-H line approximately in the middle, at ∼0.47 THz along the Γ-P line, and at ∼0.475 THz and ∼0.87 THz along the Γ-N line, respectively, approximately the halfway and near the N point. For the LA mode, avoided crossings occur at ∼1 THz about 1/4 along the Γ-H line, about 3/4 along the P-Γ line, and about 3/4 along the Γ-N line. The arbitrary k points in the Brillouin zone have no specific symmetry; hence an avoided crossing occurs inevitably for the phonon modes of a

crystal. The optic and acoustic phonon modes exchange their characters when they interact due to avoided crossing, which leads to the formation of the hybrid modes [34]. The degree of hybridization between the filler and the framework phononic modes, and thus the avoided crossing properties, depend significantly on the filler [35,36]. A weak coupling between the filler and the framework results in independent vibrations of the filler atoms, i.e., the so-called Einstein oscillators. Hence the phonon dispersion compared to that of the empty framework structure remains almost unchanged. Our calculations showed that light fillers such as Na and K have weak interactions with Si atoms and form local avoided crossings. However, the heavy fillers such as Rb, Cs, Sr, Ba, and even Ca, which are large enough to fill the framework, cause strong hybridization between acoustic modes of the framework and the filler modes leading to extended avoided crossings. In fact, the extended avoided crossings of Rb, Cs, Sr, and Ba open a gap in the phonon dispersion. The symmetry-avoided crossings between the dispersing host phonon modes and nondispersing filler phonon modes of the same symmetry can reduce the thermal conductivity in three ways. First, they can reduce the phonon group velocity. Second, they can remarkably increase the phonon scattering by reducing the phonon lifetimes [11,12], and third, the filler atoms, as we will show, reduce the Debye temperature resulted from the reduction of the phonon bandwidth. The strength of the filler-framework hybridization partly determines the relative strength of these effects.

Figure 2 compares the partial density of states of fillers in X_8Si_{46}-VIII clathrates (X = Na, K, Rb, Cs, Ca, Sr, Ba). It is evident that all fillers reside in the region of low frequency phonon density of states. The fillers exhibit three distinct features. First, the formation of the phonon band gap for four of them (Rb, Cs, Sr, and Ba) is again observed near 2 THz frequency. Second, all fillers exhibit sharp characteristics corresponding to the localized phonon modes. The localized states indicate that the motion of the fillers is independent of the host Si atoms, and fillers behave like Einstein oscillators. It is notable that for the Rb and Cs cases, unlike Sr and Ba, the gap appears slightly above the 2 THz frequency. The third is a different trend in the change of the framework partial phonon DOS with respect to the filler mass. The partial DOS of filled Si_{46} with light atoms Na, K, and Ca has similar shape as in pristine Si_{46}. However, for the case of the heavy fillers, Rb, Cs, Sr, and Ba, at low frequency, the shape of the partial density of states of the framework changes and becomes surprisingly similar to that of the filler. This can be seen by similar peaks in both partial DOSs although their intensity is different. This indicates strong interaction of the heavy fillers with the host atom. Moreover, the stronger intensity of the partial DOS of the heavy fillers compared to that of the host shows that the acoustic modes are occupied mainly by the heavy fillers.

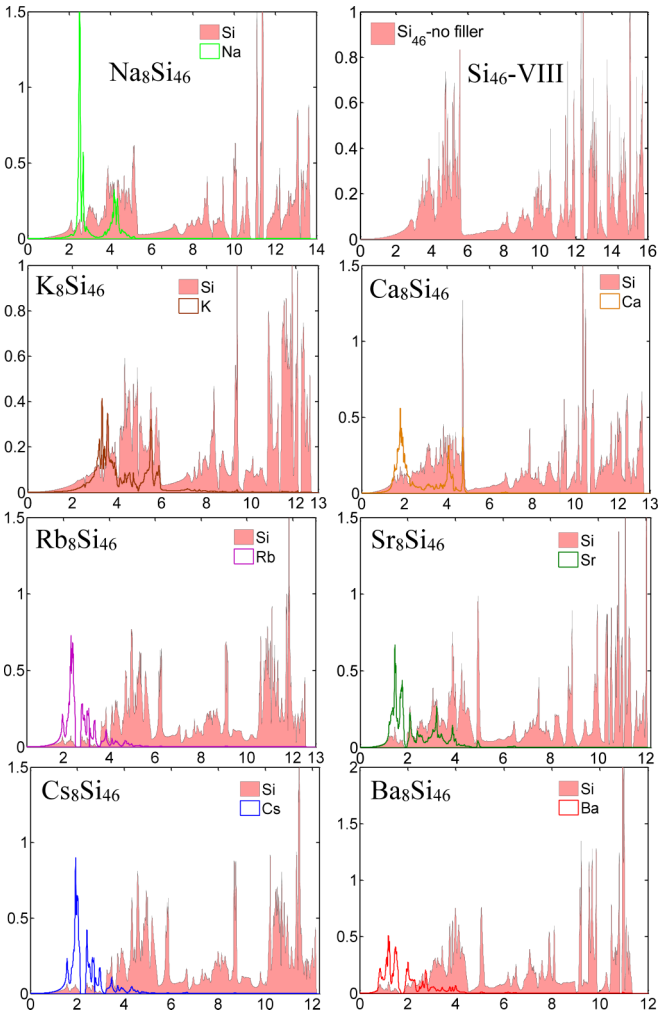

FIG. 2. Comparison between the partial phonon density of states of fillers in X_8Si_{46} (X = Na, K, Rb, Cs, Ca, Sr, and Ba).

B. Elastic properties

The elasticity of the framework, which is a function of the bonding stretch, presents another important degree of freedom that allows for the hybridization of the filler and the framework vibrations. The bonding strength also affects the Debye temperature. To find out the effect of the fillers on the strength of the filler-framework interaction, we calculated the elastic properties of X_8Si_{46} (X = Na, K, Rb, Cs, Ca, Sr, Ba) materials. Table I presents our calculated values for the elastic constants, elastic moduli, Poisson ratio, longitudinal, transverse, and mean sound velocities and the Debye temperature. It can be seen that the elastic constants, elastic moduli, sound velocities, and Debye temperature all decrease upon the insertion of the filler. These reductions suggest that the insertion of the filler in the framework makes the lattice less rigid. The reduction is more for the heavier fillers. Therefore, according to the Slack formula, $\kappa_l \propto \theta_D^{3/2} \propto B^{3/2}$, the reduction of the bulk modulus (B) (by 73% in Ba_8Si_{46}-VIII) must lead to the reduction of the thermal conductivity.

For better visualization, the mean phonon group velocity and the Debye temperature were extracted for all the studied structures and represented in Fig. 3. Figure 3 depicts the phonon group velocity and the Debye temperature versus atomic mass of the filler atoms. The filler atoms are in two groups of alkali and alkaline earth elements. Two clear trends are observed. First, as the atomic mass rises, the Debye temperature and the phonon group velocity decrease. Second, this decrement for the alkaline earth atoms is larger than that of the alkali atoms. In fact, Ba filler lowers the

TABLE I. Predicted elastic constants C_{ij}, bulk modulus B, shear modulus G, factor of anisotropy (no unit), and Young's moduli E, E_{100}, and E_{111}, Poisson's ratios, longitudinal, transverse, and mean sound velocities, and Debye temperatures for X_8Si_{46} (X = Na, K, Rb, Cs, Ca, Sr, and Ba). The results for the clathrates with alkali and alkaline earth filler atoms are in blue and brown, respectively. The data for Si_{46} were adopted from Ref. [1].

Filler	Void	Na	K	Rb	Cs	Ca	Sr	Ba
C_{11} (GPa)	149.3	133.8	128	117.9	95.1	120.3	98.07	79.1
C_{12}(GPa)	49.2	50	45.4	43.8	47.4	62	62.2	74.4
C_{44} (GPa)	46.8	41.9	38.5	35.7	24.7	31.2	13.46	8.9
B (GPa)	82.6	77.9	72.9	68.5	63.3	81.4	74.14	75.9
G (GPa)	48.1	41.9	39.6	36.2	24.4	30.4	15.1	5.2
C_a	1.03	1	1.03	1.02	0.99	0.97	1.12	1.1
E(GPa)	120.8	106.5	100.6	92.4	64.8	81.1	42.43	15.3
E_{100} (GPa)	124.9	106.6	104.2	94.2	63.5	78.1	49.82	35
E_{111} (GPa)	118.2	106.5	98.3	91.2	65.7	83.1	38.1	26
v	0.24	0.27	0.27	0.275	0.33	0.33	0.41	0.45
V_l (ms^{-1})	8395	7575	7184	6304	5291	6925	5560	5724
V_t (ms^{-1})	4807	4239	4032	3511	2668	3457	2225	1674
V_s (ms^{-1})	5196	4718	4487	3910	2992	3879	2521	1908
θ_D (K)	549	522	490	424	322	429	276	150

most the phonon group velocity and the Debye temperature among all the studied alkali and alkaline earth atoms. For Ba_8Si_{46}-VIII, the transverse acoustic (TA) and longitudinal acoustic (LA) phonon group velocities drop almost by 75% and 42%, respectively. With respect to the reduction of the phonon group velocity by 1/3 for the case of Ba filler, Ba would be the best filler for lowering the thermal conductivity of Si_{46}-VIII clathrate structure.

C. Participation and atomic participation ratios

To shed light into the characteristics of the spectral weight of the filler atoms, and their effect on the localization of the phonons, the frequency dependent participation ratio (PR) and the atomic participation ratio (APR) of the phonon modes were calculated for all the selected materials. In particular, the PR of the phonon modes can be employed to quantify the level of phonon localization. The PR determines the degree of participation of the constituent atoms in a given phonon mode and enables us to discriminate between the coherent displacements of all atoms as collective excitations and the rattling modes as localized excitations [37]. The PR value of the propagative phonon modes, in which most of the atoms participate, is close to 1. The PR value of the diffusive phonon modes is around ∼0.5–0.6, which are the characteristic of the amorphous materials. Finally, the PR value of the localized phonon modes in which a few atoms participate is ∼0.2 [38]. The PR is defined by the following equation:

$$p(\omega_q) = \frac{\left(\sum_{i=1}^{N} |\mathbf{u}_i(\omega_q)|^2\right)^2}{N \sum_{i=1}^{N} |\boldsymbol{u}_i(\omega_q)|^4} \tag{7}$$

in which $\mathbf{u}_i = \boldsymbol{e}_i(\boldsymbol{q})/\sqrt{M_i}$ are the atomic amplitudes. The $\boldsymbol{e}_i(\boldsymbol{q})$ are the phonon polarization vectors and the M_i are the masses of the atoms. Figure 4 depicts the participation ratios for all materials investigated in this study. The participation ratio of all the cases represents some similar features. First, all patterns have been shifted towards the lower PRs with respect to that of the empty framework, which indicates that the fillers develop more localized characteristics in phonon transport. Second, upon loading the fillers into the Si framework, additional nonpropagative phonon modes with very small PR (∼0.15) are observed.

For better understanding, Fig. 5 summarizes the results of PR calculations by comparing the PR values of empty Si_{46}-VIII framework and Ba_8Si_{46}-VIII clathrate structure. In the low frequency region of the acoustic modes as shown in Fig. 5, three sharp features of density of states at 1, 1.75, and 2.1 THz frequencies can be identified as localized Ba vibrations. Moreover, below the gap region and at 1 THz, the host silicon atoms display small DOS peaks which overlap with that of the Ba vibrations. This inspection substantiates the interaction of the acoustic modes with the localized vibrations through the resonant hybridization.

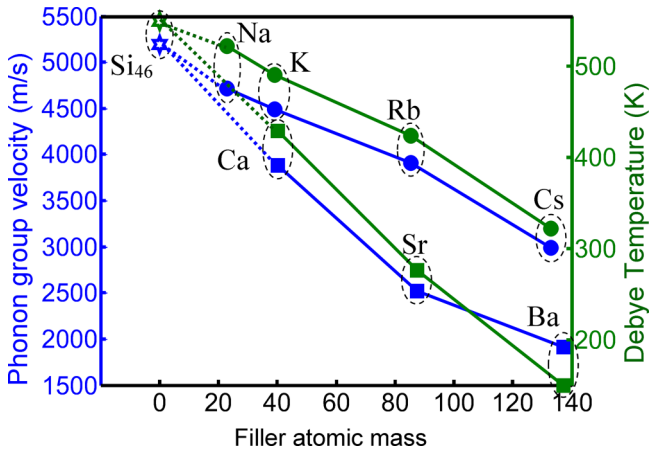

FIG. 3. The phonon group velocity and Debye temperature versus atomic mass of filler atoms. The data of Si_{46}-VIII has been added for comparison. Green and blue curves refer to Debye temperature and phonon group velocity, respectively. The dotted lines are for better demonstration of the trends.

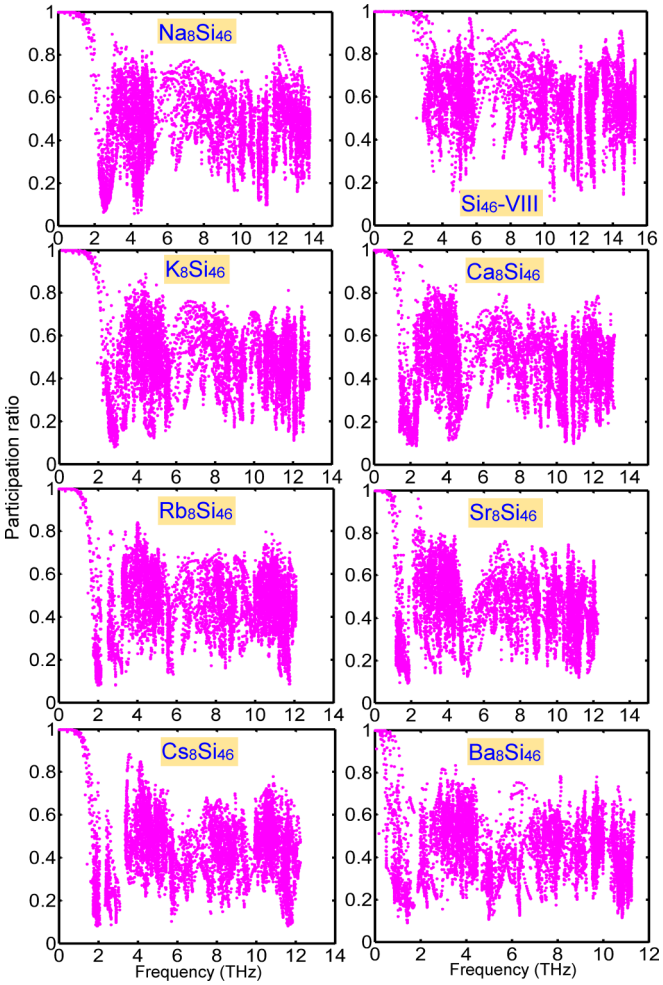

FIG. 4. Comparison of the calculated participation ratios for the filled alkali and alkaline earth atoms and empty Si_{46}-VIII frameworks.

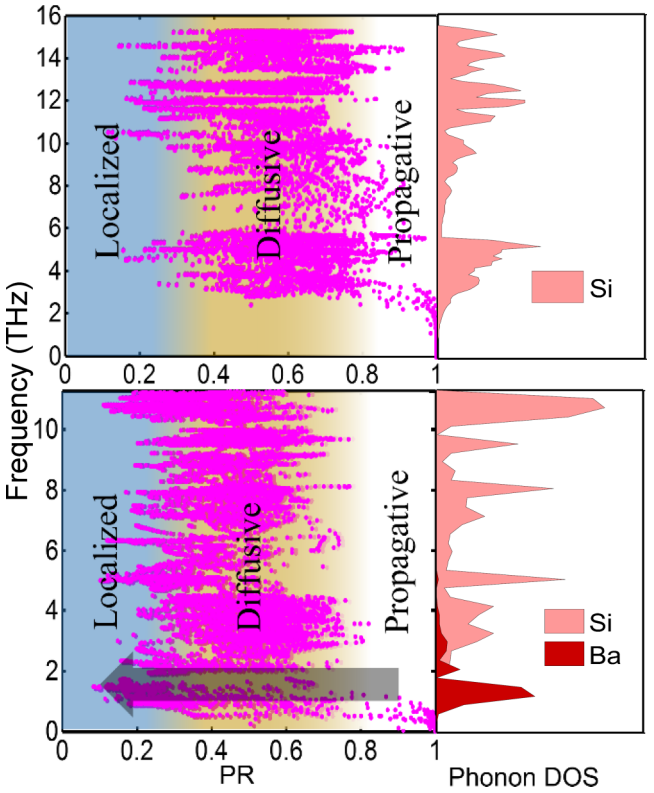

FIG. 5. Participation ratios for phonons and the partial phonon density of states for Si_{46} and Ba_8Si_{46}. The smaller values of PR correspond to more localized phonon modes. The arrow shows the phonons transformed from propagative to diffusive and localized modes due to Ba in Ba_8Si_{46}.

It can be seen that loading the Ba atoms in the framework shifts the PR to lower values, which indicates higher degree of localization in the phonon modes. Therefore the phonon transport is transformed from propagative and diffusive regimes to the localized one. Like type-I clathrates, there is a strong hybridization with the heavy filler (especially Ba) modes, which leads to phonon modes with low group velocity that essentially do not propagate and can reduce the thermal conductivity [13]. The Si_{46} phonon dispersion contains acoustic modes with a PR close to 1 within the 0–3.6 THz frequency range. In comparison, the corresponding frequency range for Ba_8Si_{46} is limited to 0–0.2 THz, which is more than an order of magnitude smaller. It is important to note that, according to the phonon dispersion in Fig. 1 and the atom projected phonon DOS in Fig. 5, the depressed acoustic phonon modes in Ba_8Si_{46} are populated mostly by Ba atoms. Therefore Si atoms have little contribution in the heat transfer via the acoustic modes. The transfer of heat conduction from Si atoms to Ba atoms in Ba_8Si_{46} and the replacement of the propagative modes by diffusive modes upon loading the filler atoms can contribute to the reduction of the thermal conductivity. A similar transfer to the localized transport regime also occurs for the other filler atoms according to the PR results. Figure 5 also shows a zero PR region around 2 THz, which corresponds to the phonon bandgap observed in Fig. 1.

An interesting measure which can quantify the degree of participation of different atoms in a specific phonon mode and can describe the localization of phonons is called atomic participation ratio (APR) and is defined as

$$p_i(\omega) = \frac{|\mathbf{u}_i(\omega_q)|^2}{\sqrt{N\sum_{i=1}^{N}|\mathbf{u}_i(\omega_q)|^4}}. \quad (8)$$

This quantity separates the contributions of different types of atoms existent in the lattice for a particular frequency [13] offering insight about the phonon localization in the studied clathrates. Figures 6 and 7, respectively, present the APR patterns of silicon frameworks X_8Si_{46}-VIII, where X = Na, K, Rb, Cs, Ca, Sr, Ba, and the APR of fillers. All the studied fillers show a similar effect on the APR pattern of the Si framework of X_8Si_{46}-VIII, where X = Na, K, Rb, Cs, Ca, Sr, and Ba. For all the fillers, the whole APR pattern makes a shift towards lower-frequency range, and this effect is maximized for the Ba case. All the fillers demonstrate a similar APR pattern with little discrepancies. As the atomic mass of the filler increases, an APR gap is developed above the acoustic phonon modes. In case of Cs, two gaps are observed. It is notable that the APR of Ba atoms in the region of the acoustic phonon modes is very narrow.

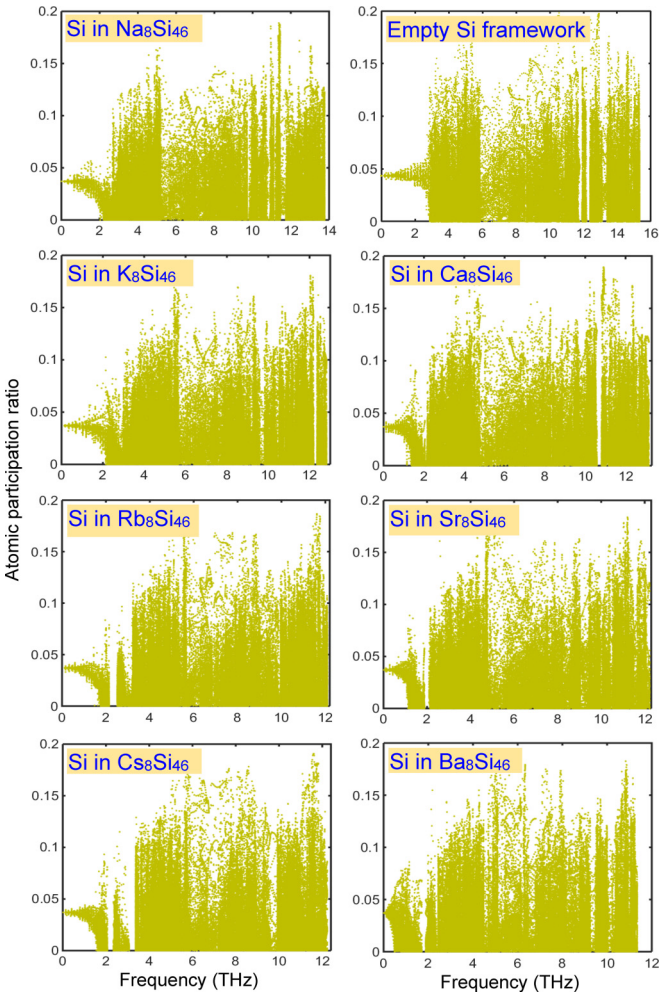

FIG. 6. The effect of fillers on the APR of the X_{46}Si-VIII framework, where X = Na, K, Rb, Cs, Ca, Sr, and Ba.

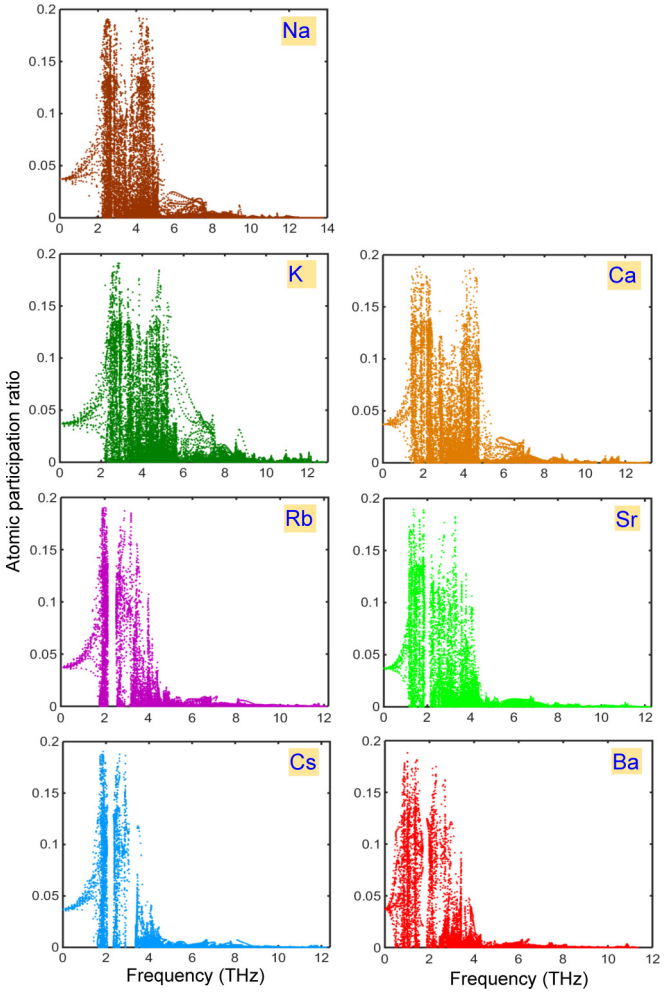

FIG. 7. Comparison of the APR of fillers inside the Si_{46}-VIII framework. Only the contributions of fillers have been presented in this figure and the contribution of Si host atoms have been removed for better visualization.

According to Fig. 1, the Ba_8Si_{46} vibration frequencies within the 0–1.8 THz range correspond to LA and TA phonon modes. Figure 8 shows that below 0.15 THz, Si and Ba atoms have similar motions with a constant APR, which corresponds to the acoustic modes. In the 0.15–1.7 THz frequency window, the contribution of Ba atoms in acoustic phonon modes increases while that of the Si atoms decreases. In this frequency range, Si atoms are almost localized and only Ba atoms participate in the acoustic phonon modes. For frequencies between 1.7 and 1.85 THz, a zero APR region appears, which indicates that for the mentioned frequency range no acoustic phonon is formed either by Si or Ba atoms. It is observed that beyond the APR gap up to 2.4 THz, Ba atoms still dominantly contribute to phonon modes. Another APR gap appears within the 2.4–2.45 THz range, which implies that the avoided crossings are stretched into the optical phonon region. The optical phonons in the frequency range of 2.45–2.9 THz are associated to both Si and Ba atoms. At higher frequencies, the displacements of Si atoms mainly form the optical phonons, and the contribution from Ba atoms decreases. The APR analysis corroborates that Si atoms contribute to only a small region of the acoustic modes, and they become localized quickly as the phonon frequency goes above 0.15 THz, which

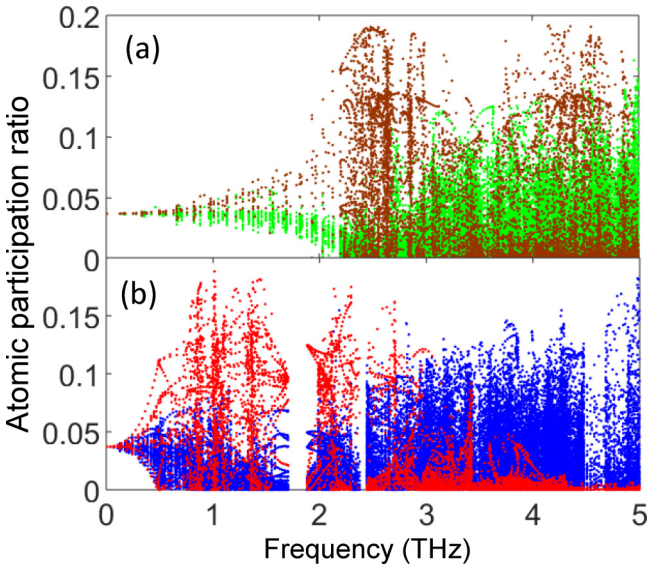

FIG. 8. Atomic participation ratio of (a) Si (green) and Na (brown) in Na_8Si_{46}-VIII, and (b) Si (blue) and Ba (red) in Ba_8Si_{46}-VIII.

indicates that Si and Ba atoms are not entangled. However, at low phonon frequency (<0.15 THz), most of the Si and Ba atoms vibrate with similar frequency. It should be noted that these are the phonons that contribute dominantly in heat conduction. The APR analysis of the other fillers indicate that the existence and size of the APR gap depends on the mass of the filler. The larger the filler atomic mass, the more probability of the formation of a gap, and the bigger the APR gap.

IV. CONCLUSIONS

In summary, the following conclusions can be drawn regarding the effect of the alkali and alkaline earth filler atoms in Si_{46}-VIII: (i) Si atoms in the pristine and the filled Si_{46} with light atoms (Na, K, and Ca) contribute nearly equally in the low frequency acoustic phonons. The shape of the partial density of states for Si atoms is not affected by the light fillers either. (ii) When the framework is filled with heavy atoms (Rb, Sr, Cs, and Ba), the acoustic modes are mainly populated by the fillers and the partial phonon DOS of the framework is suppressed significantly. Moreover, the framework partial phonon DOS at low frequency takes similar shape (although with much lower intensity) as that of the heavy fillers. (ii) The alteration of the vibrational modes from Si to guest atoms transforms the energy transport from propagative to a mixed diffusive and localized regime. This change is more significant for the case of heavier guests. Furthermore, the frequency at which this mode transfer occurs is smaller for the heavier fillers. (iv) Heavy fillers (Rb, Sr, Cs, and Ba) showed formation of phonon band gaps in the frequency range of the acoustic modes of the pristine Si_{46} lattice, which is not observed in the phonon dispersion of the light elements. (v) The filler insertion depressed the phonon bandwidth, reduced the Debye temperature, and reduced the phonon group velocity, all of which should lead to reduction of the thermal conductivity. These changes were larger for the case of heavier guests. (vi) The strong interaction of the heavy fillers and the host atoms, endorsed by the APR trends and the avoided crossing of the phonon modes, indicates that the rattler concept is not adequate to describe the lattice dynamics in these clathrates and has been overgeneralized. The host-filler interaction increases with the filler mass.

ACKNOWLEDGMENTS

This study is partially based upon work supported by Air Force Office of Scientific Research (AFOSR) under Contract No. FA9550-12-1-0225 and the National Science Foundation (NSF) under Grants No. EEC-1160483, No. ECCS-1351533, and No. CMMI-1363485. The authors would like to thank Tandy Supercomputing Center for the generous amounts of computer time on the high performance computing center.

[1] P. Norouzzadeh, C. W. Myles, and D. Vashaee, J. Phys.: Condense. Matter. **25**, 475502 (2013).
[2] V. Keppens, D. Mandrus, B. Sales, B. Chakoumakos, P. Dai, R. Coldea, M. Maple, D. Gajewski, E. Freeman, and S. Bennington, Nature (London) **395**, 876 (1998).
[3] R. P. Hermann, R. Jin, W. Schweika, F. Grandjean, D. Mandrus, B. C. Sales, and G. J. Long, Phys. Rev. Lett. **90**, 135505 (2003).
[4] M. M. Koza, M. R. Johnson, R. Viennois, H. Mutka, L. Girard, and D. Ravot, Nat. Mater. **7**, 805 (2008).
[5] J. L. Feldman, D. J. Singh, I. I. Mazin, D. Mandrus, and B. C. Sales, Phys. Rev. B **61**, R9209 (2000).
[6] N. Bernstein, J. L. Feldman, and D. J. Singh, Phys. Rev. B **81**, 134301 (2010).
[7] B. Huang and M. Kaviany, Acta Mater. **58**, 4516 (2010).
[8] M. Zebarjadi, K. Esfarjani, J. Yang, Z. F. Ren, and G. Chen, Phys. Rev. B **82**, 195207 (2010).
[9] A. D. Ritchie, M. B Johnson, J. F Niven, M. Beekman, G. S. Nolas, J. Gryko and M. A. White, J. Phys.: Condens. Matter. **25**, 435401 (2013).
[10] H. Euchner, S. Pailhès, L. T. K. Nguyen, W. Assmus, F. Ritter, A. Haghighirad, Y. Grin, S. Paschen, and M. de Boissieu, Phys. Rev. B **86**, 224303 (2012).
[11] M. Christensen, A. B. Abrahamsen, N. B. Christensen, F. Juranyi, N. H. Andersen, K. Lefmann, J. Andreasson, C. R. H. Bahl, and B. B. Iversen, Nat. Mater. **7**, 811 (2008).
[12] T. Tadano, Y. Gohda, and S. Tsuneyuki, Phys. Rev. Lett. **114**, 095501 (2015).
[13] S. Pailhès, H. Euchner, V. M. Giordano, R. Debord, A. Assy, S. Gomès, A. Bosak, D. Machon, S. Paschen, and M. de Boissieu, Phys. Rev. Lett. **113**, 025506 (2014).
[14] P. Norouzzadeh, J. S Krasinski, C. W Myles, and D. Vashaee, Phys. Chem. Chem. Phys. **17**, 8850 (2015).
[15] P. Norouzzadeh, C. W. Myles, and D. Vashaee, Sci. Rep. **4**, 7028 (2014).
[16] G. Kresse and J. Furthmüller, Phys. Rev. B **54**, 11169 (1996).
[17] J. P. Perdew, K. Burke, and M. Ernzerhof, Phys. Rev. Lett. **77**, 3865 (1996).
[18] H. Monkhorst and J. Pack, Phys. Rev. B **13**, 5188 (1976).
[19] M. Methfessel and A. T. Paxton, Phys. Rev. B **40**, 3616 (1989).
[20] E. N. Nenghabi and C. W. Myles, Phys. Rev. B **78**, 195202 (2008).
[21] K. Parlinski, *Software Phonon, version 4.28* (2005). http://wolf.ifj.edu.pl/phonon/Public/phrefer.html.
[22] MedeA Materials Exploration and Design Analysis Software (Materials Design, Inc.) v 2.12. Available online at https://www.materialsdesign.com/medea.
[23] D. R. Hamann, X. Wu, K. M. Rabe, and D. Vanderbilt, Phys. Rev. B **71**, 035117 (2005).
[24] M. J. Mehl, J. E. Osburn, D. A. Papaconstantopoulos, and B. M. Klein, Phys. Rev. B **41**, 10311 (1990).
[25] A. V. Hershey, ASME J. Appl. Mech. **21**, 236 (1954).
[26] E. Kröner, Z. Phys. **151**, 504 (1958).
[27] R. Hill, Proc. Phys. Soc. London **65**, 349 (1952).
[28] L. Vitos, *Computational Quantum Mechanicals for Materials Engineers* (Springer-Verlag, London, 2007).
[29] H. M. Ledbetter, J. Appl. Phys. **44**, 1451 (1973).
[30] G. Grimvall, *Thermophysical Properties of Materials* (North-Holland, Amsterdam, 1999).
[31] J. H. Page, S. Yang, Z. Liu, M. L. Cowan, C. T. Chan, and P. Sheng, Z. Kristallogr. **220**, 859 (2005).
[32] D. A. Broido, L. Lindsay, and T. L. Reinecke, Phys. Rev. B **88**, 214303 (2013).

[33] J. Dong, O. F. Sankey, and C. W. Myles, Phys. Rev. Lett. **86**, 2361 (2001).

[34] H. Schober, H. Itoh, A. Klapproth, V. Chihaia, and W. F. Kuhs, Eur. Phys. J. E **12**, 41 (2003).

[35] D. M. Rowe, *Thermoelectric Handbook: Macro to Nano* (CRC Press, 2005).

[36] T. Takabatake, K. Suekuni, T. Nakayama, and E. Kaneshita, Rev. Mod. Phys. **86**, 669 (2014).

[37] J. Hafner and M. Krajci, J. Phys. Condens. Matter **5**, 2489 (1993).

[38] Y. M. Beltukov, V. I. Kozub, and D. A. Parshin, Phys. Rev. B **87**, 134203 (2013).